Ratcheting Fatigue in Full-Scale Piping Elements

F. Hara
Science University of Tokyo,
Dept. of Mechanical Engineering, 1-3, Kagurazaka, Shinjuku-ku, Tokyo 162, Japan
H. Shibata
Institute of Industrial Science,
University of Tokyo, 22-1, Roppongi 7-chome, Minato-ku, Tokyo 106, Japan

We experimentally investigated characteristics of low-cycle mechanical ratcheting fatigue in full-scale piping elements--e.g., straight pipes (6B Sch 40), long elbows (6B Sch 40), tees (6B Sch 40), branched pipes (6B Sch 40, 1/2B Sch 40), and reducers (6B Sch 40, 4B Sch 40)--under steady internal pressure equivalent to an S_m value and conditions of oscillatory bending or torsional load. We also gathered valuable information on ratcheting damage modes and fatigue life for assessing failure probability in main piping systems of a nuclear plant undergoing a very large earthquake.

Piping elements used were mainly 6B Sch 40 (ID=150 mm, t=7.1 mm), of STS 42 steel. The steady internal load was supplied by water pressure of 105 Kgf/cm^2. The two external oscillatory loads--bending and torsion--were each sinusoidal (1 Hz) and stationary random (0 to 1 Hz). Experiments showed the kind and location of ratcheting damage in piping elements; the εt to N_f relation; difference in fatigue life between sinusoidal and stationary random loads; and influence of loading involving bending and torsion.

We obtained the following major results.

1) Ratcheting fatigue damage modes--rupture location in piping elements and swelling due to ratcheting--were observed and a qualitative interpretation of ratcheting damage modes was made, i.e., rupture due to ratcheting occurred where local strain produced by both steady internal and dynamic external loads was maximum.

2) Fatigue damage modes were the same for stationary random and sinusoidal loads.

3) Fatigue life characteristics were found for maximum local strain εt and load cycle N_f up to rupture, i.e.,

$$\left(\frac{\varepsilon t}{12.5}\right)^{2.5} N_f = 1$$

4) For stationary random loads, the number of peaks in random input up to which pipe rupture occurred was 2 to 2.5 times larger than for sinusoidal input when the rms of peak values of stationary input was equal to sinusoidal input amplitude.

1. Introduction

Mechanical ratcheting deformation--progressive increase of plastic deformation due to simultaneous loading of steady pressure and cyclic bending or torsional load--has been studied by several researchers [1 - 4] to clarify mechanical characteristics of the ratcheting process. They used small test pieces and simplified loading conditions to avoid experimental complexities, however, and little work has been done on such fatigue in large-scale piping elements. Udoguchi et al [5] demonstrated safety margins for piping elements like elbows and tees under cyclic loading (bending, torsion, and both combined). Fujita et al [6] evaluated endurance of a 3B piping system including elbows and tees from vibration test data obtained for extra large acceleration (3G).

We experimentally investigated characteristics of low-cycle mechanical ratcheting fatigue in full-scale piping elements--straight pipes (6B Sch 40), long elbows (6B Sch 40), reducers (6B Sch 40, 4B Sch 40), tees (6B Sch 40), and branched pipes (6B Sch 40, 1/2B Sch 40) --under steady internal pressure equivalent to an S_m value and cyclic bending or torsional load. We also obtained information on the characteristics of random fatigue in ratcheting deformation in the pipe elements we studied.

2. Experiments

2.1 Test Pipe Elements

Test pipe specimens used were of STS 42 (Japanese standards, equivalent to ASME 106 Grade B) carbon steel. Tables 1 and 2 show the chemical content of the STS 42 steel and mechanical properties.

We tested straight pipes, long elbows, reducers, tees, and branched pipes. Figs. 1 (a) to (e) show test specimen dimensions of these elements. The key dimension was an outer diameter Do=165.2 mm, and pipe wall thickness t=7.1 mm.

2.2 Test Facilities

An electric oil hydraulic actuator with a maximum dynamic capacity of ±10 tons and ±100 mm strokes under a cyclic velocity of 0.8 Hz was used for loading dynamic force on test specimens. The connecting rod transferring the dynamic load was designed to avoid test specimen displacement influence on loading direction. Steady internal pressure was supplied with water using a small manual pump connected to a 330-liter accumulator. Photos 1 and 2 show an view of the test facility and a test pipe specimen (tee) set in the test facility.

2.3 Test Conditions

Dynamic load mode. We used two load modes--sinusoidal and random cyclic. The cyclic velocity of sinusoidal wave loading was 1 Hz, except for torsional load on straight pipe specimens, when loading was 0.5 Hz sinusoidally cyclic. Table 3 shows the combination of loading and test specimens, where M: bending load; Mi: in-plane bending load; Mo: out-of-plane bending load; T: torsional load; S: sinusoidal waves; and R: random waves.

Fig. 2 shows frequency characteristics for random loading. Most frequency components were concentrated from 0 to 0.6 Hz.

Steady internal pressure. Internal pressure in test piping specimens was kept constant at 105 Kgf/cm^2, equivalent to the S_m value of STS 42 carbon steel.

Loading conditions. We used a displacement controlled test where displacement amplitude of the loading end of test pipe specimens was kept constant during testing. Load direction in the initial cycle was kept the same for all sinusoidal load mode tests.

2.4 Instrumentation

To obtain quantitative information on the mechanical ratcheting fatigue process, we measured, during testing: 1) strain of a specimen's outer surface at 13 points located rather densely near a projected rupture point; 2) displacement amplitude of the loading end of test pipes; 3) changes in internal pressure; 4) load supplied by the actuator; 5) temperature at a projected rupture point on the specimen's outer surface; and, after rupture, 6) outer diameter of the piping specimen suffering permanent deformation from ratcheting fatigue; 7) size of cracks on the outer surface of test specimens; and 8) photographs of cracks and pipe swelling.

Before starting each test, we measured a specimen's outer diameter at several places to evaluate pipe swelling due to ratcheting fatigue.

3. Results

3.1 Fatigue Mode

Photo 3 shows the sharp exhaust of water pressurized to 105 Kfg/cm^2 when a crack reached the outer surface of the specimen. We defined this condition as "rupture."

For cases of sinusoidal loading, the following rupture modes occurred in full-scale piping elements.

Straight pipe--bending. Photo 4 shows a large crack appearing on the specimen's surface and swelling in the neighborhood of the crack penetrating the pipe wall and occurring along a line where both the bending stress produced by the external load and the local bending deformation generated by the mechanical ratcheting mechanism were very large. Both sides of the pipe in the loading direction were locally swollen in about 5% excess of their original diameter. At the other two sides, pipe diameter was slightly enlarged.

Straight pipe--torsion. Photo 5 shows a large circumferential rupture. The pipe's diameter was enlarged rather uniformly over the whole test specimen. Some small axial cracks on the pipe's surface were also observed.

Elbow--in-plane bending. Photo 6 shows a view of crack size and location. The lip of the crack is sharply concave. The elbow showed a large swelling perpendicular to the loading direction, while the elbow showed slight shrinkage in an in-plane direction.

Elbow--out-of-plane bending. As Photo 7 shows, two cracks appeared on the 45° circumferential line of the elbow, which was uniformly, radially swollen.

Reducer--bending. Photo 8 shows circumferential crack size and location, indicating that the thinner pipe suffered severe ratcheting damage in the region connecting to the reducer, which was apparently unaffected.

Reducer--torsion. Photo 9 shows a large circumferential crack, and its location, describing the mechanical condition of ratcheting fracture due to cyclic torsion load. Fine axial cracks which did not penetrate the pipe wall were also observed. The thinnner pipe was rather uniformly swollen the same as the straight pipe, above.

Tees--in-plane bending. Photo 10 shows severe swelling. Two cracks formed perpendicular to the lines where the cross of the tee joined the tee stem. Lips of cracks were also concave similar to that for elbow in-plane loading. Many circumferential wrinkles appeared on the concave surface of the tees.

Tees--out-of-plane bending. A large trapezoidal crack appeared in the region where the tee connected to the branched straight pipe, or tee stem, as shown in Photo 11. Ratcheting swelling occurred over the whole area of tees tested.

Branched pipe--out-of-plane bending. Photo 12 shows a severe rupture in the connecting region of the smaller pipe.

3.2 Fatigue Characteristics

Fig. 3 shows the relationship between a local maximum strain εt (peak to peak value in %) near the penetrating crack at the initial cycle of loading for each test specimen and the cycle number where the ratcheting fracture occurs to exhaust pressurized water, i.e.,

$$\left(\frac{\varepsilon t}{12.5}\right)^{2.5} N_f = 1$$

This figure also contains the ASME design curve for low-cycle fatigue, which is almost 50% lower than the ratcheting fatigue value.

3.3 Random Fatigue Characteristics

Table 4 summarizes results of the random ratcheting fatigue test--load mode, the rms of the test specimen's loading end displacement, and the cycle number of fatigue limit.

Local maximum strain corresponding to the rms value of displacement was estimated from the experimental relation between strain and displacement. Estimated local maximum strain (peak to peak value in %) can evaluate ratcheting fatigue life $\hat{N}_f$ number from Fig. 3. Table 5 shows estimated strain and fatigue life. Ratio $N_{fr}/\hat{N}_f$ indicates random fatigue life increase, which is about 2 to 2.5 times larger than the normal low-cycle fatigue.

4. Conclusions

We explored ratcheting fatigue failure modes occurring in full-scale piping elements--straight pipes, elbows, reducers, tees, and branched pipes--and obtained a well-demonstrated relation between maximum local strain εt and fatigue life N_f. Random fatigue life for this ratcheting failure in full-scale piping elements was evaluated as being twice as long as the life obtained from the sinusoidal loading test.

Acknowledgments

This research was done under the EDR program. The authors wish to thank Professor Yasuhide Asada of the University of Tokyo for his invaluable suggestions concerning the experimental work, and to express their deep appreciation to the members of the EDR research committee for their kind assistance.

References

[1] COFFIN, JR, L. F., Trans. ASME, Ser. D, 82-3 (1960-9), 671.

[2] UDOGUCHI, Y., et al, Trans. JSME, 42-359 (1976-7), 1982.

[3] TANAKA, K., et al, Trans. JSME, 42-358 (1976-6), 1685.

[4] YOSHIDA, F., et al, Trans. JSME, 43-571 (1977-7), 2500.

[5] UDOGUCHI, Y., et al, Trans, 34d SMiRT, K7/5, (1973).

[6] FUJITA, K., et al, Trans. JSME, 44-386 (1978-10), 343.

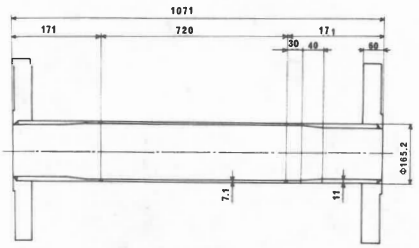

Fig. 1 (a) Straight pipe

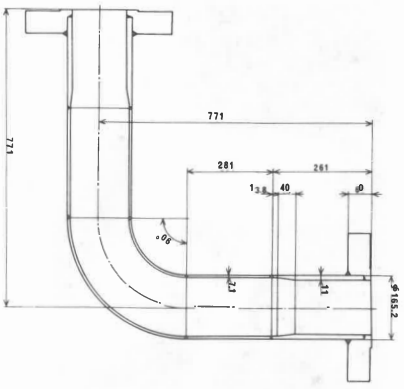

Fig. 1 (b) Elbow

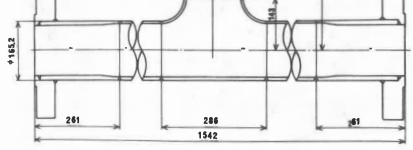

Fig. 1 (c) Tee

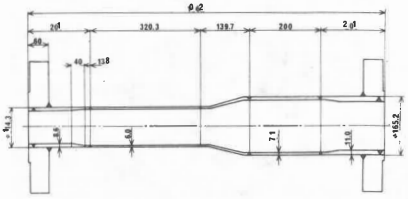

Fig. 1 (d) Reducer

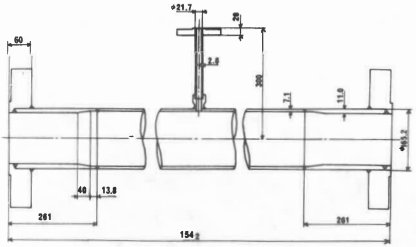

Fig. 1 (e) Branched pipe

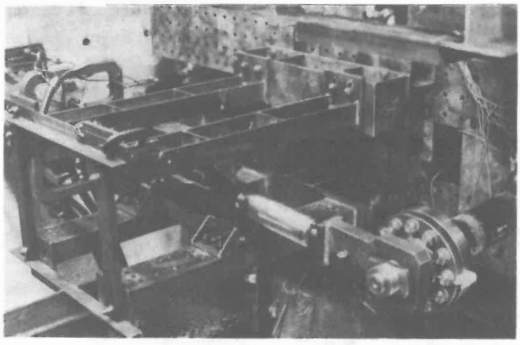

Photo 1 Test facility

Photo 2 Tee set in test facility

Photo 5 Straight pipe--torsion

Photo 3 Water exhaust at rupture

Photo 6 Elbow--in-plane bending

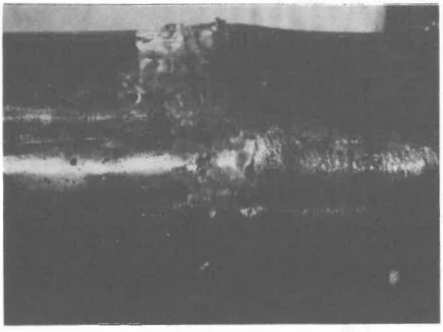

Photo 4 Straight pipe--bending

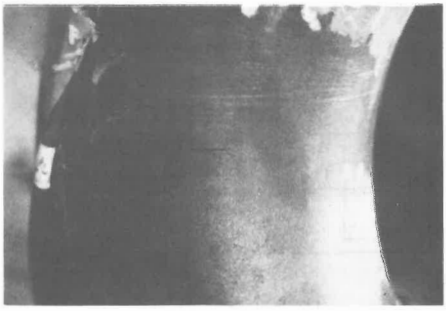

Photo 7 Elbow--out-of-plane bending

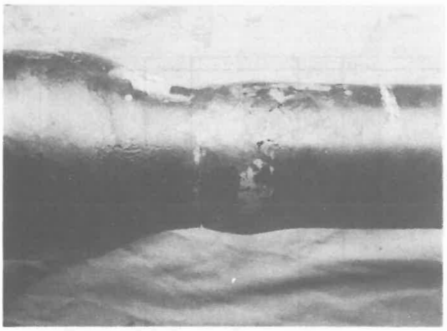

Photo 8 Reducer--bending

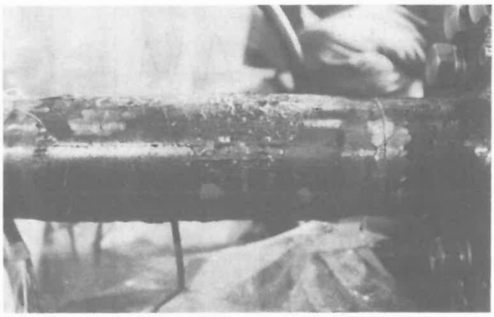

Photo 9 Reducer--torsion

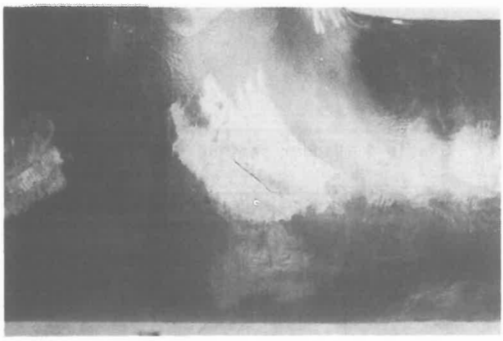

Photo 10 Tee--in-plane bending

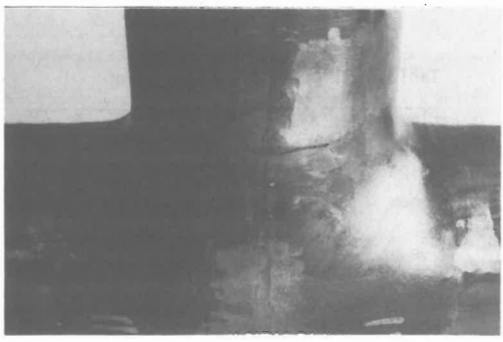

Photo 11 Tee--out-of-plane bending

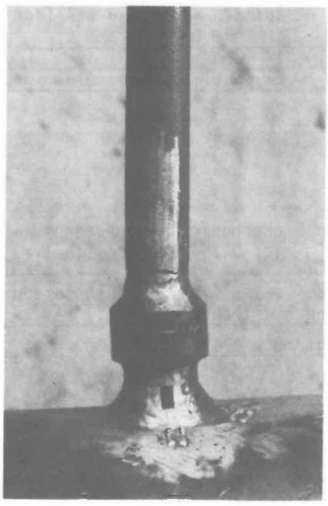

Photo 12 Branched pipe--bending

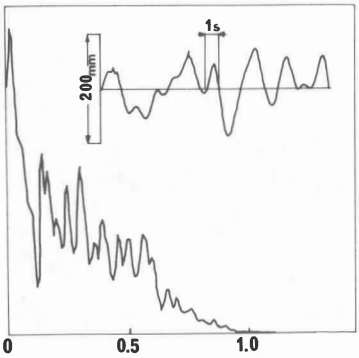

Fig. 2 PSD of random input

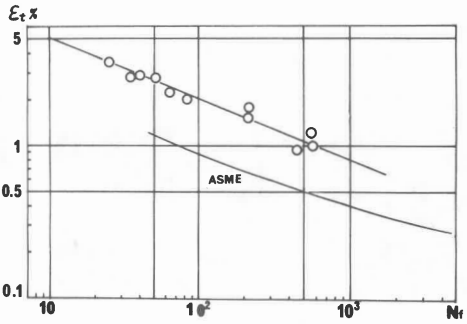

Fig. 3 Ratcheting fatigue life

Table 1 Chemical content of STS 42 carbon steel (%)

C	Si	Mn	P	S	Cu
0.20	0.21	0.51	0.0016	0.02	0.01

Table 2 Mechanical properties of STS 42 carbon steel

Yield strength	Tensile strength	Elongation (%)
30 Kgf/mm²	47 Kgf/mm²	38

Table 3 Piping elements and loading modes

Straight pipe	(M,S)	(M,R)	(T,S)
Elbow	(Mi,S)	(Mi,R)	(Mo,S)
Reducer	(M,S)	(T,S)	
Tee	(Mi,S)	(Mo,S)	(Mo,R)
Branched pipe	(Mo,S)	(Mo,R)	

Table 4 Random fatigue test results

Element	Load mode	Displacement rms (mm)	N_{fr}
Straight pipe	Bending	20.9	330
Elbow	In-plane bending	36.4	220
Tee	Out-of-plane bending	27.6	339
Branched pipe	Bending	20.4	317

Table 5 Estimated fatigue life

Element	Load mode	$\hat{\varepsilon}t$ (%)	$\hat{N}_f$	$N_{fr}/\hat{N}_f$
Straight pipe	Bending	2.1	130	2.5
Elbow	In-plane bending	1.5	220	2.4
Tee	Out-of-plane bending	1.6	170	2.0
Branched pipe	Bending	1.5	332	0.96